

# Electrogenerated Chemiluminescence of Solutions, Films, and Nanoparticles of Dithienylbenzothiadiazole-Based Donor–Acceptor–Donor Red Fluorophore. Fluorescence Quenching Study of Organic Nanoparticles

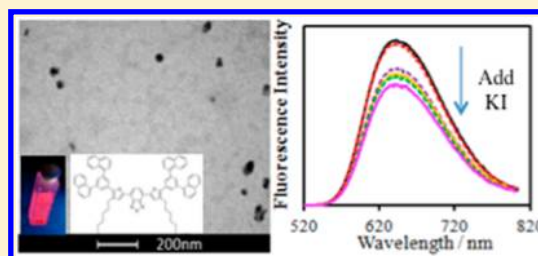
Mei Shen,<sup>†,§</sup> Xu-Hui Zhu,<sup>‡</sup> and Allen J. Bard<sup>\*,†</sup>

<sup>†</sup>Center for Electrochemistry, Department of Chemistry and Biochemistry, University of Texas at Austin, 105 East 24th Street Station A5300, Austin, Texas 78712-1224, United States

<sup>‡</sup>State Key Laboratory of Luminescence Materials and Devices, Institute of Polymer Optoelectronic Materials and Devices, South China University of Technology, Guangzhou 510640, China

## Supporting Information

**ABSTRACT:** We report here the electrochemistry, spectroscopy, and electrogenerated chemiluminescence (ECL) from a solution, film, and nanoparticles (NPs) of a red-emitting dithienylbenzothiadiazole molecular fluorophore [4,7-bis(4-(*n*-hexyl)-5-(3,5-di(1-naphthyl)phenyl)-thiophen-2-yl)-2,1,3-benzothiadiazole, **1a**], which has a donor–acceptor–donor configuration. In addition, the quenching of the fluorescence of the organic NPs by KI was investigated. The **1a** film and NPs exhibit two absorbance peaks at 350 and ~504 nm that are red-shifted compared to those of **1a** dissolved in solution (340 and 486 nm). Fluorescence quenching of **1a** NPs does not follow a linear Stern–Volmer relationship; i.e., the fluorescence emission with excitation wavelength at either 350 or 504 nm decreased with increasing concentration of KI. Static quenching and heterogeneity related to the size distribution of the **1a** NPs are proposed to explain the nonlinearity. A lifetime of  $4.49 \pm 0.04$  ns was found for **1a** organic NPs in water saturated with N<sub>2</sub>. After addition of KI, the fluorescence lifetime decreased to 3.1 ns. The fluorescence emission of **1a** film/NPs is red-shifted (~17 nm) compared with that of **1a** solution in dichloromethane (DCM). Solution ECL was generated in DCM through an annihilation reaction, while film and NP ECL could be generated in water through oxidation with a coreactant, tri-*n*-propylamine (TPrA). A film of **1a** with thickness of 100–900 nm was prepared by drop-casting **1a** in DCM on fluorine-doped tin oxide, and the ECL of the **1a** film was found in phosphate-buffered saline solution with TPrA. Both **1a** in solution and the **1a** film produce strong ECL ( $I_{\text{film}} = 0.14I_{\text{solution}}$ ). The ECL spectrum of **1a** in solution, produced by electron-transfer annihilation of the reduced and oxidized forms, consists of a single peak with maximum emission at about  $637 \pm 4$  nm, ~20 nm red-shifted from its fluorescence, while the ECL spectrum of **1a** produced by reaction with TPrA consists of a single peak with maximum emission at  $642 \pm 3$  nm, a 10 nm red shift compared with the fluorescence of **1a** film. Organic fluorescent **1a** NPs were prepared by a reprecipitation method in water saturated with N<sub>2</sub>, and they were characterized by transmission electron microscopy, absorbance, fluorescence, and ECL. Strong ECL was also generated from the organic NPs in water by reduction with K<sub>2</sub>S<sub>2</sub>O<sub>8</sub> coreactant.



## INTRODUCTION

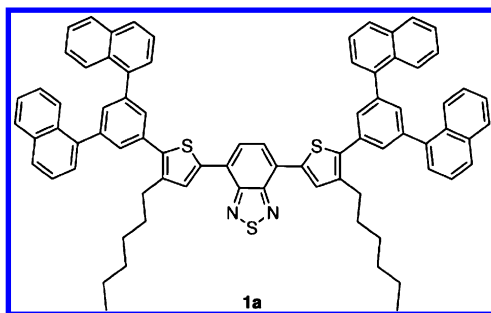
We report here the electrogenerated chemiluminescence (ECL) of a dithienylbenzothiadiazole derivative, a red fluorophore (compound **1a**<sup>1</sup>), in different states—solution, film, and nanoparticle (NP)—as well as the fluorescence quenching of **1a** NPs by iodide ion. The ECL of film and NPs were studied in phosphate-buffered saline (PBS) buffer and water, respectively. Compound **1a** has a 2,1,3-benzothiadiazole moiety as the electron acceptor as a center connected directly to two donors at the ends. Each donor is a thiophene moiety substituted in position 2 by 3,5-di(1-naphthyl)phenyl and in position 3 by *n*-hexyl. Compound **1a** is reported to have a high photoluminescence (PL) quantum yield in both solution and solid states (44% of Rhodamine B in solution and 62% in the

solid measured in an integrating sphere under 325 nm laser excitation).<sup>1</sup>

ECL is the process whereby species generated at electrodes undergo energetic electron-transfer reactions to form excited states that emit light.<sup>2</sup> ECL can be generated through two dominant pathways, namely the annihilation and coreactant pathways.<sup>3,4</sup> In annihilation ECL, emission of light could be either from the reaction of radical anions and cations generated near the electrode surface (singlet or S-route) or from formation of triplets followed by triplet–triplet annihilation (T-route). Coreactants are also used in ECL studies when one of the generated radical species is unstable or cannot be

Received: December 13, 2012

Published: May 30, 2013



generated within the solvent window.<sup>3</sup> Here we find the ECL of a **1a** solution results from the S-route following electrochemical reduction and oxidation, and the ECL of **1a** films and NPs results from a coreactant reaction.

Classically, most ECL studies of various fluorophores were carried out in organic solvents.<sup>5–13</sup> ECL has also been generated from films of fluorophores.<sup>14–24</sup> Among the studies of film ECL, only a few studies were performed in aqueous solution, and these were limited to films with tris(2,2'-bipyridine)ruthenium(II) derivatives<sup>19–22,24</sup> or J-aggregates of amphiphilic cyanine dye.<sup>23</sup> We report here an ECL study of the film of **1a** in aqueous PBS buffer, where the fluorophore is totally insoluble in water. We also compare the emission in both states.

Organic NPs have recently received attention because of the large available range of different molecular structures, the diversity and flexibility in material synthesis and preparation, and the ability to tailor their binding affinity toward various materials.<sup>25</sup> Moreover, fluorescent organic NPs are expected to find a wide variety of applications, such as nanosized organic light-emitting diodes (OLEDs), biologics,<sup>26</sup> inks, toners, drugs, and cosmetics.<sup>27</sup> Very few studies have reported the ECL of organic NPs.<sup>28,29</sup> The quantum confinement or fine size effects shown for semiconductor and metal NPs<sup>30–33</sup> are less likely to show size-dependent optical properties in organic NPs with much weaker intermolecular interactions, although small effects have been reported for sizes ranging from a few tens to a few hundred nanometers. Fluorescence quenching of semiconductor NPs has been studied.<sup>34–39</sup> Despite numerous studies on the spectral properties of organic NPs, fluorescence quenching of organic NPs by halide ions, as described here, has not been studied previously.

## EXPERIMENTAL SECTION

**Materials.** Anhydrous dichloromethane (CH<sub>2</sub>Cl<sub>2</sub> or DCM) and tripropylamine (TPrA) were obtained from Aldrich (St. Louis, MO) and transferred directly into a helium atmosphere drybox (Vacuum Atmospheres Corp., Hawthorne, CA) without further purification. Electrochemical-grade tetra-*n*-butylammonium hexafluorophosphate (TBAPF<sub>6</sub>) was obtained from Fluka and used as received. Tris(2,2'-bipyridine)ruthenium(II) perchlorate (Ru(bpy)<sub>3</sub>ClO<sub>4</sub>) was obtained from GFS Chemicals, Inc. (Powell, OH). Compound **1a** was synthesized as reported.<sup>1</sup> Characterization details (NMR) are contained in this reference.

**Organic Film and Nanoparticle Preparation.** The **1a** film was prepared by drop-casting 25  $\mu$ L of 0.5 mM **1a** in DCM on fluorine-doped tin oxide (FTO) and allowing it to air-dry. **1a** NPs were prepared by injecting drop-by-drop 2 mL of 50  $\mu$ M **1a** in THF into 20 mL of water (in an 80–88 °C water bath) under stirring using a 100  $\mu$ L syringe. After injection, the solution was heated to 90–95 °C on a hot plate, and stirring was continued for another 10 min; the hot plate was then turned off while stirring continued for another 10 min.

**Characterization.** Cyclic voltammograms (CVs) were obtained on a CH Instruments electrochemical workstation (CHI 660, Austin,

TX). Digital simulations of CV were performed using Digisim software (Bioanalytical Systems). Absorbance spectra were obtained on an Agilent Technologies UV-Vis Chem Station. Fluorescence spectra of **1a** in solution were collected on a QuantaMaster spectrofluorimeter (Photon Technology International, Birmingham, NJ). The excitation source was a 70 W xenon lamp (LPS-220B lamp power supply), and the excitation and emission slits were set to 0.5 mm (2 nm bandwidth). The fluorescence spectra and lifetime measurements of **1a** NPs were recorded on a spectrofluorimeter (FluoroLog-3, Horiba Jobin Yvon). The excitation source was a 450 W xenon arc lamp for spectra measurements and pulsed Nano LED-482 nm for lifetime measurements. The quenching studies were performed in water saturated with N<sub>2</sub>. Thickness of the **1a** film was measured with an NT9100 Optical Profiler (Veeco, Plainview, NY).

The ECL spectra were obtained on a Princeton SPEC-10 instrument using a charge-coupled device (CCD) camera (Trenton, NJ) cooled to –100 °C with an Acton SpectraPro-150 monochromator (Acton, MA) as a detector. The wavelength scales of the CCD camera and grating system were calibrated using a Hg/Ar per-ray lamp from Oriel (Stratford, CT).

For study of **1a** in solution, solutions were prepared inside the glovebox. For measurements made outside of the box, the electrochemical cell was closed with a Teflon cap that had a rubber O-ring to form an airtight seal. Stainless steel rods driven through the cap formed the electrode connections. The electrochemical cell consisted of a coiled Pt wire (0.5 mm in diameter) as a counter electrode, a Ag wire (0.5 mm in diameter) as a quasi-reference electrode, and a Pt disk inlaid in glass bent at a 90° angle (for the disk to face the light detector) as a working electrode. After each experiment, the potential of the Ag wire was calibrated with ferrocene (taken as 0.342 V vs SCE).<sup>40</sup> Before each experiment, the working electrode was polished on a felt pad with 1, 0.3, and 0.05  $\mu$ m alumina (Buehler, Ltd., Lake Bluff, IL) and sonicated in Milli-Q deionized water. The counter and reference electrodes were cleaned by rinsing and sonicating in acetone, water, and ethanol. Finally, all the electrodes were rinsed with acetone, dried in an oven, and transferred into a glovebox. For study of **1a** NPs, the same counter and working electrodes were used and cleaned as described above, but a Ag/AgCl reference electrode was used. For study of **1a** film, the same counter electrode was used and cleaned as described above, an Ag/AgCl reference electrode was used, and the working electrode was a FTO electrode with **1a** film on it. Spectroscopic experiments were done in a 1 cm path length quartz cell. Absorbance of **1a** film was measured on a quartz slide with quartz as reference. Transmission electron microscopy (TEM) was performed with a Tecnai transmission electron microscope (FEI Co., Hillsboro, OR). A TEM sample was prepared by drop-casting 10  $\mu$ L of **1a** NPs in water on carbon-film-coated Cu TEM grids; vacuum was applied during the sample-drying process.

## RESULTS AND DISCUSSION

**ECL of **1a** in Solution.** A CV of **1a** in CH<sub>2</sub>Cl<sub>2</sub> is shown in Figure 1, where one reduction and two oxidation waves were observed. The CV results can be rationalized from the chemical

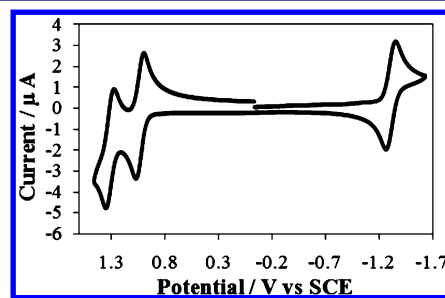


**Figure 1.** CV of 0.5 mM **1a** in DCM with 0.1 M TBAPF<sub>6</sub>. Scan rate = 100 mV/s; area of electrode = 0.028 cm<sup>2</sup>.

structure of **1a**, which comprises a 2,1,3-benzothiadiazole moiety as the reduction center (A-group) and two bulky substituted thiophene end groups as donor groups (D-group). Digital simulations of the experimental CVs for reduction and oxidation were performed (Supporting Information, Figures S1 and S2). The best fit for the CV simulation suggests a single 1e reduction with  $E_{\text{red}}^{\circ} = -1.18 \pm 0.005$  V vs SCE,  $D = 6 \times 10^{-6}$  cm<sup>2</sup>/s, and  $k^{\circ} = 0.6 \times 10^{-3}$  cm/s, and two 1e oxidations with  $E_{\text{oxi},1}^{\circ} = 1.01 \pm 0.005$  V vs SCE,  $E_{\text{oxi},2}^{\circ} = 1.24 \pm 0.005$  V vs SCE,  $D = 6 \times 10^{-6}$  cm<sup>2</sup>/s, and  $k^{\circ} = 0.02$  cm/s. The smaller heterogeneous electron-transfer rate constant for the reduction compared with that for the oxidation is consistent with previous results where the reduction center was blocked by the two bulky end groups.<sup>41</sup>

Figure 2 shows the ECL, absorbance, and PL spectra of **1a** in CH<sub>2</sub>Cl<sub>2</sub>. The ECL spectrum was generated by pulsing the

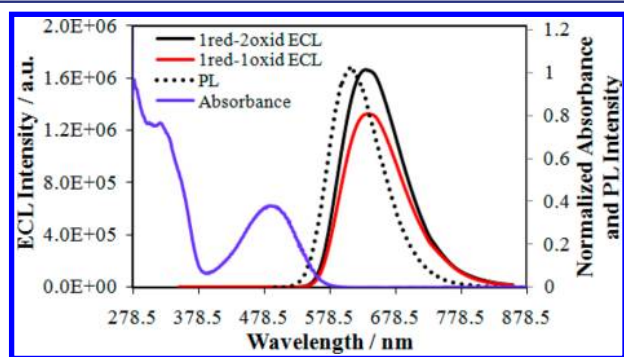


**Figure 2.** ECL spectra of 0.5 mM **1a** in 0.1 M TBAPF<sub>6</sub> in DCM obtained by pulsing between 80 mV past the reduction peak potential and two different anodic potentials, 80 mV past the first oxidation peak potential, and 80 mV over the second oxidation peak potential, as well as normalized absorbance and normalized fluorescence or PL spectrum of 7  $\mu$ M **1a** in DCM. ECL spectra were integrated for 30 s using a 0.5 mm slit width. Excitation wavelength for fluorescence emission = 485 nm.

electrode potential between the reduction and the two possible oxidations. The wavelengths for maximum absorbance, PL, and ECL are shown below in Table 2. Compound **1a** has a Stokes shift of  $129 \pm 4$  nm and shows some absorbance within the wavelength range of PL and ECL. ECL spectrum is red-shifted  $\sim 22$  nm compared to the PL spectrum; such a shift has been observed in many ECL studies of other compounds<sup>9–11</sup> and is often the result of an inner filter effect in ECL at the higher concentrations employed compared to PL and slight differences in the different instruments used in ECL and PL. Stronger ECL was generated from the reaction of radical anion and radical dication, indicating stability of the radical dication. The ECL of **1a** was compared to that of Rubpy (quantum efficiency is about 5% in MeCN),<sup>42,43</sup> a widely investigated ECL molecule, as well as that of the previously reported molecule **1b**,<sup>9</sup> and the results are shown in Table 1. The ECL quantum efficiency is defined as the ratio of the number of photons emitted to the number of annihilations between the radical anion and radical cation of the fluorophore.<sup>42</sup> Measurement of the absolute efficiency is experimentally difficult, so relative efficiencies are usually reported. The comparison of ECL, made in terms of maximum intensity and integrated area of ECL spectra in Table 1, demonstrates strong ECL generated from compound **1a**, although smaller than those of the previously reported molecule **1b** and Rubpy.

**Table 1.** Maximum ECL Emission Wavelength  $\lambda_{\text{max}}^{\text{ECL}}$  of **1a** and Its Relative Intensity with Respect to Rubpy and **1b** under Conditions of Figure 2

pulsing potentials	$\lambda_{\text{max}}^{\text{ECL}}$ (nm)	relative intensity (%)		integrated area (%)	
		vs <b>1b</b> <sup>a</sup>	vs Rubpy <sup>b</sup>	vs <b>1b</b> <sup>a</sup>	vs Rubpy <sup>b</sup>
1red-1oxid	637 $\pm$ 4	(21 $\pm$ 5)	(17 $\pm$ 3)	(22 $\pm$ 5)	(42 $\pm$ 6)
1red-2oxid	637 $\pm$ 4	(41 $\pm$ 5)	(31 $\pm$ 3)	(19 $\pm$ 4)	(33 $\pm$ 3)

<sup>a</sup>Calculated by comparing the  $I_{\text{max}}^{\text{ECL}}$  and integrated area of ECL spectrum of **1a** with those of **1b** in DCM. <sup>b</sup>Calculated by comparing the  $I_{\text{max}}^{\text{ECL}}$  and integrated area of ECL spectrum of **1a** with those of Rubpy in MeCN. For reduction–first oxidation of **1a**, comparison was made with reduction–first oxidation of **1b** and first reduction–oxidation of Rubpy; for reduction–second oxidation of **1a**, comparison was made with reduction–second oxidation of **1b** and second reduction–oxidation of Rubpy. Absolute ECL quantum efficiency of Rubpy is 5% in MeCN.<sup>42,43</sup>

**ECL of **1a** Film and NPs in Aqueous Solution.** A **1a** film was prepared on a transparent electrode (FTO), and the CV of the film is shown in the Supporting Information (Figure S3A,B). The background-subtracted CV shows an integrated charge of  $1.5 \times 10^{-4}$  C from the 25  $\mu$ L of 0.5 mM **1a** deposited, indicating that about 12% of the deposited material is electroactive. The ECL properties of **1a** film on FTO were studied in aqueous PBS buffer solution with TPrA as the coreactant. The thickness of the films measured using a profilometer was 100–900 nm. Figure 3a shows that very strong ECL was generated from a **1a** film when it was scanned from 0 to 2 V vs SCE. As a comparison, Figure 3b is the result from a bare FTO electrode in PBS buffer solution in the presence of TPrA (background). No ECL was generated in the absence of a **1a** film (Figure 3b). Because **1a** is insoluble in water, there is little chance that ECL could be generated from dissolved **1a**.

**1a** NPs were prepared using a coprecipitation method.<sup>29</sup> Thus-prepared **1a** NPs are colorless to the eye under ambient light (Figure 4A), while they fluoresce red under UV-lamp irradiation (Figure 4B). The organic NPs were characterized by TEM (Figure 4C); Figure 4D shows the size distribution. While the **1a** NPs have a wide size distribution, they are mostly of an average size of  $\sim 10$  nm. The broad size distribution might be related with the size of the droplet from the syringe during injection, the time of injection, and the temperature of the water during injection.

The absorbance of the **1a** NPs, film in water, and **1a** in a solution in DCM is shown in Figure 5a. The **1a** NPs and film have very similar absorbance maxima at 504 nm, 18 nm red-shifted compared to the absorbance maximum at 486 nm of the **1a** solution in DCM. As can be seen from Figures 5b and 5c, the fluorescence emission maxima of **1a** NPs and film are the same, both at  $632 \pm 5$  nm, around 17 nm red-shifted compared to the fluorescence maximum of solution at  $615 \pm 4$  nm.

The ECL properties of **1a** organic NPs were studied by applying  $-2$  V for 10 min with 100 mM K<sub>2</sub>S<sub>2</sub>O<sub>8</sub> as a coreactant, resulting in the spectrum shown in Figure 5b. Quite strong ECL was generated from **1a** NPs, with a much broader spectrum than that of **1a** in solution, perhaps because of the wide size distribution of the **1a** NPs.

The maximum wavelengths of absorbance, fluorescence emission, and ECL for **1a** film, NPs, and solution as discussed

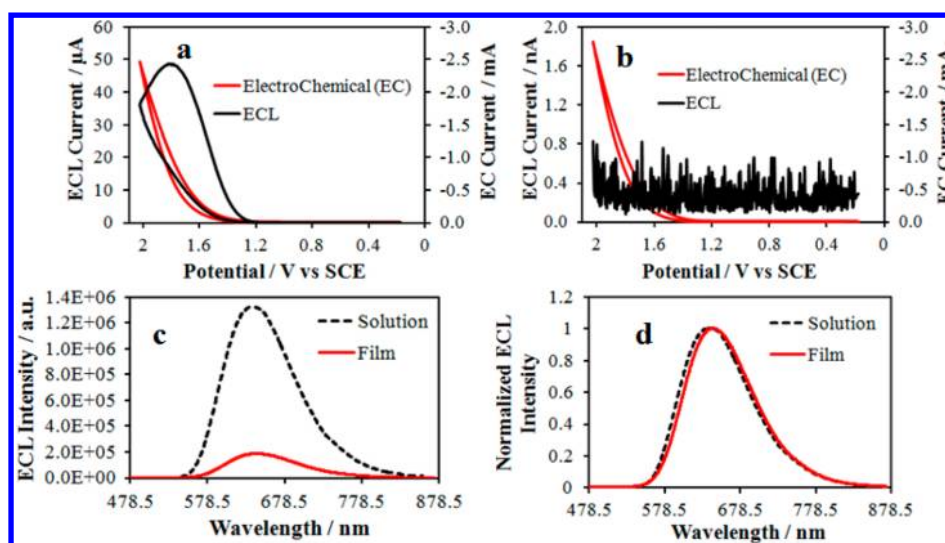


**Figure 3.** ECL coupled with CV (electrochemical) of **1a** film on FTO in PBS buffer with 20  $\mu\text{L}$  of TPrA (a) and bare FTO in PBS buffer with 20  $\mu\text{L}$  of TPrA (b). ECL spectra (c) and normalized ECL spectra (d) of 0.5 mM **1a** in 0.1 M TBAPF<sub>6</sub> in DCM obtained by pulsing between 80 mV past the reduction peak potential and 80 mV past the first oxidation peak potential (solution) and **1a** film on FTO in 8 mL of PBS buffer with 20  $\mu\text{L}$  of TPrA as coreactant. ECL of **1a** film was generated by scanning from 0 to 2 V vs SCE with a scan rate of 0.5 V/s for 20 cycles.

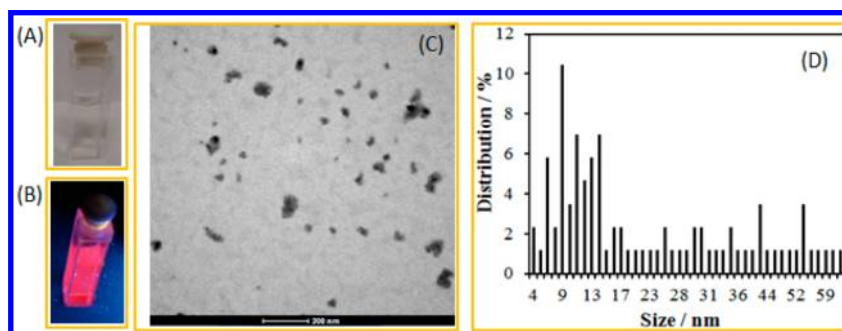


**Figure 4.** Photographs of **1a** organic nanoparticles in water under (A) ambient and (B) UV light. TEM results (C) and size distribution (D) of **1a** organic NPs. The density of **1a** NPs used in the TEM is  $\sim 10^{-5}$  g/cm<sup>3</sup>.

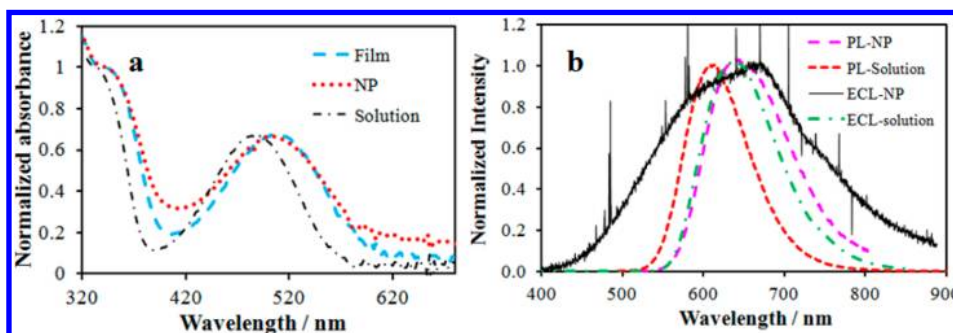


**Figure 5.** (a) Normalized absorbance of 7  $\mu\text{M}$  **1a** solution in DCM, **1a** film, and **1a** NPs in water. (b) Normalized PL spectrum of **1a** NPs in water, and ECL spectrum of **1a** NPs in water generated with 100 mM K<sub>2</sub>S<sub>2</sub>O<sub>8</sub> as coreactant. Normalized PL and ECL spectra of **1a** solution in DCM are shown for comparison.

above are summarized in Table 2. In summary, NPs and film have similar absorbance and emission maxima, both  $\sim 17$  nm red-shifted compared to those of solution. Note that the ECL, absorbance, and fluorescence spectra of the film and solution were measured with the same instrument. It would be interesting to compare the results we observed here with those from the literature. Seixas de Melo et al.<sup>44</sup> studied the absorption and fluorescence emission of oligomers in solution (at 293 and 77 K) and in films. They found that the absorbance and fluorescence wavelengths were red-shifted in the film and

**Table 2.** Maximum Absorbance, PL, and ECL Emission Wavelengths of **1a** in Dichloromethane (Solution), **1a** Film, and **1a** Nanoparticles in Water

form of <b>1a</b>	$\lambda_{\text{max}}^{\text{abs}}$ (nm)	$\lambda_{\text{max}}^{\text{PL}}$ (nm)	$\lambda_{\text{max}}^{\text{ECL}}$ (nm)
solution	486	615 $\pm$ 4	637 $\pm$ 4
film	504	632 $\pm$ 5	642 $\pm$ 3
NPs	504	632 $\pm$ 5	—

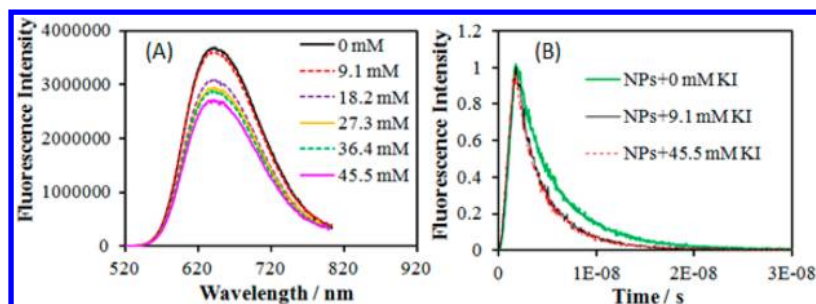


**Figure 6.** (A) Fluorescence spectra of **1a** organic NPs without KI and in the presence of KI at different concentrations. (B) Fluorescence decay profiles of **1a** organic NPs before and after addition of KI. The decay profiles for KI concentrations ranging from 9.1 to 45.5 mM are overlapped. Error in fluorescence intensity = 1%; error in fluorescence lifetime = 0.9%.

in the frozen low-temperature solution compared with the room-temperature solution. A monolayer of surfactant derivative of  $\text{Ru}(\text{bpy})_3^{2+}$  also showed red-shifted ECL compared with solution-phase  $\text{Ru}(\text{bpy})_3^{2+}$ .<sup>19</sup> The small red-shift of the spectra from solution to film and NPs may be attributed to the loss of conformational freedom, causing a lowering of the energy gap between the HOMO and LUMO<sup>44,45</sup> or electron stacking.<sup>46,47</sup>

#### Quenching of **1a** Organic Nanoparticles by KI.

Quenching of the PL of organic NPs by dissolved species has not been studied previously, and we thought it of interest to report some preliminary experiments with **1a** NPs. Quenching of NPs is largely a NP surface phenomenon, so the quenching depends strongly on NP size. Since the size distribution of the NPs described here is large, quantitative conclusions are not possible (see eqs S3 and S4). Fluorescence quenching of the **1a** NPs by KI was studied, and plots of fluorescence intensity and lifetime upon addition of KI are shown in Figure 6. Figure 6A shows a decrease of fluorescence intensity upon addition of increasing concentrations of KI in water. The fluorescence lifetime also decreased with addition of 9.1 mM KI, from 4.45 ns without KI to 3.1 ns with it (Figure 6B). However, with the addition of more KI, while the overall fluorescence intensity decreased, the lifetime was essentially unchanged.

Collisional (dynamic) quenching of fluorescence follows the Stern–Volmer equation,

$$I_0/I = 1 + k_q\tau_0[Q] \quad (1)$$

where  $I_0$  and  $I$  are fluorescence intensities in the absence and presence of quencher, respectively,  $k_q$  is the rate constant of quenching,  $\tau_0$  is the lifetime of the fluorophore in the absence of the quencher, and  $[Q]$  is the concentration of the quencher.<sup>48–50</sup> This equation predicts a linear plot of  $I_0/I$  or  $\tau_0/\tau$  vs  $[Q]$  for a homogeneously emitting solution.<sup>51</sup> Figure S6 shows plots of  $I_0/I$  and  $\tau_0/\tau$  vs  $[Q]$ , where the quenching is nonlinear. Nonlinear Stern–Volmer plots are often found in macromolecules, e.g., proteins and NPs,<sup>49,52–59</sup> and these are often attributed to static quenching (e.g., complexation of the fluorophore and quencher) and heterogeneity of the fluorophore.<sup>58</sup>  $I_0/I$  does not follow the same trend as  $\tau_0/\tau$ , i.e.,  $I_0/I \neq \tau_0/\tau$  (Figure S6), indicating that static quenching is possible. The absorbance spectra of **1a** NPs also change upon addition of KI (Figure S7). This suggests that adsorption of iodide to the NP surface can cause quenching. Although inorganic NPs are very different than the organic NPs under consideration here, there are parallels to these studies, e.g., CdSe NPs,<sup>39</sup> wherein NPs in general do not follow a collisional quenching model but rather suggest that iodide anions only

quench near surface molecules of the NP, but do not affect the core. However, a more quantitative treatment requires monodispersity rather than the broad distribution that usually characterizes organic NPs, where a summation of the individual size NP quenching must be employed (see eqs S3 and S4).

## CONCLUSIONS

Strong ECL was generated from solution, solid films, and nanoparticles of a red, highly fluorescent molecular dye, **1a**. Films and NPs show red-shifted absorbance and fluorescence emission spectra compared to those of the solution. **1a** in solution produces strong ECL by annihilation, while **1a** films produce strong ECL in an aqueous PBS buffer with TPrA as a coreactant. The ECL spectrum from the NPs in an aqueous medium generated with a coreactant was much broader, which is probably related to the large size distribution of the NPs. The fluorescence of the organic **1a** NPs is quenched by KI, with evidence of both dynamic and static quenching.

## ASSOCIATED CONTENT

### Supporting Information

Simulation of CVs; CV of film, excitation spectra, and absorbance spectra of **1a** NPs upon addition of KI; equations for the calculation of quenching constant in the presence of static quenching and heterogeneity. This material is available free of charge via the Internet at <http://pubs.acs.org>.

## AUTHOR INFORMATION

### Corresponding Author

ajbard@mail.utexas.edu

### Present Address

<sup>§</sup>M.S.: Department of Chemistry, University of Illinois Urbana–Champaign, Urbana, IL 61801

### Notes

The authors declare no competing financial interest.

## ACKNOWLEDGMENTS

A.J.B. thanks Roche Diagnostics, Inc., the National Science Foundation (CHE 1111518), and the Robert A. Welch Foundation (F-0021), and X.H.Z. thanks SCUT, NSF, and MOST of China (2012ZZ0001, 51173051, 2009CB93060) for financial support of this research.

## REFERENCES

- (1) Huang, J.; Li, C.; Xia, Y.-J.; Zhu, X.-H.; Peng, J.; Cao, Y. *J. Org. Chem.* **2007**, *72*, 8580–8583.

- (2) IUPAC Compendium of Chemical Terminology, 2nd ed.; McNaught, A. D., Wilkinson, A., Eds.; Blackwell Science: Oxford, UK, 1997.
- (3) Bard, A. J. In *Electrogenerated Chemiluminescence*; Bard, A. J., Ed.; Marcel Dekker: New York, 2004.
- (4) For reviews on ECL, see: (a) Ref 3. (b) Miao, W. J. *Chem. Rev.* **2008**, *108*, 2506–2553. (c) Forster, R. J.; Bertinocello, P.; Keyes, T. E. *Annu. Rev. Anal. Chem.* **2009**, *2*, 359–385. (d) Richter, M. M. *Chem. Rev.* **2004**, *104*, 3003–3036. (e) Knight, A. W.; Greenway, G. M. *Analyst* **1994**, *119*, 879–890.
- (5) Maloy, J. T. In *Electrogenerated Chemiluminescence*; Bard, A. J., Ed.; Marcel Dekker: New York, 2004; p 159.
- (6) Keszthelyi, C. P.; Tokel-Takvoryan, N. E.; Bard, A. J. *Anal. Chem.* **1975**, *47*, 249–256.
- (7) Richter, M. M. In *Electrogenerated Chemiluminescence*; Bard, A. J., Ed.; Marcel Dekker: New York, 2004; p 306.
- (8) Tokel, N.; Bard, A. J. *J. Am. Chem. Soc.* **1972**, *94*, 2862–2863.
- (9) Shen, M.; Rodríguez-López, J.; Huang, J.; Liu, Q.; Zhu, X.-H.; Bard, A. J. *J. Am. Chem. Soc.* **2010**, *132*, 13453–13461.
- (10) Nepomnyashchii, A. B.; Bröring, M.; Ahrens, J.; Bard, A. J. *J. Am. Chem. Soc.* **2011**, *133*, 8633–8645.
- (11) Shen, M.; Rodríguez-López, J.; Lee, Y.-T.; Chen, C.-T.; Fan, F.-R. F.; Bard, A. J. *J. Phys. Chem. C* **2010**, *114*, 9772–9780.
- (12) Kapturkiewicz, A.; Herbich, J.; Nowacki, J. *Chem. Phys. Lett.* **1997**, *275*, 355–362.
- (13) Lai, R. Y.; Kong, X. X.; Jenekhe, S. A.; Bard, A. J. *J. Am. Chem. Soc.* **2003**, *125*, 12631–12639.
- (14) Buda, M. In *Electrogenerated Chemiluminescence*; Bard, A. J., Ed.; Marcel Dekker: New York, 2004; p 445.
- (15) Abruñá, H. D.; Bard, A. J. *J. Am. Chem. Soc.* **1982**, *104*, 2641–2642.
- (16) Fan, F.-R. F.; Mau, A.; Bard, A. J. *Chem. Phys. Lett.* **1985**, *116*, 400–404.
- (17) Richter, M. M.; Fan, F.-R. F.; Klavetter, F.; Heeger, A. J.; Bard, A. J. *Chem. Phys. Lett.* **1994**, *226*, 115–120.
- (18) Nambu, H.; Hamaguchi, M.; Yoshino, K. *J. Appl. Phys.* **1997**, *82*, 1847–1852.
- (19) Zhang, X.; Bard, A. J. *J. Phys. Chem.* **1988**, *92*, 5566–5569.
- (20) Obeng, Y. S.; Bard, A. J. *Langmuir* **1991**, *7*, 195–201.
- (21) Sato, Y.; Uosaki, K. *J. Electroanal. Chem.* **1995**, *384*, 57–66.
- (22) Rubinstein, I.; Bard, A. J. *J. Am. Chem. Soc.* **1980**, *102*, 6641–6642.
- (23) Walker, E. K.; Vanden Bout, D. A.; Stevenson, K. J. *J. Phys. Chem. C* **2011**, *115*, 2470–2475.
- (24) Dennany, L.; O'Reilly, E. J.; Forster, R. J. *Electrochem. Commun.* **2006**, *8*, 1588–1594.
- (25) Suk, J.; Bard, A. J. *J. Solid State Electrochem.* **2011**, *15*, 2279–2291.
- (26) (a) Yao, H.; Ashiba, K. *RSC Adv.* **2011**, *1*, 834–838. (b) Jagannathan, R.; Irvin, G.; Blanton, T.; Jagannathan, S. *Adv. Funct. Mater.* **2006**, *16*, 747–753.
- (27) Asahi, T.; Sugiyama, T.; Masuhara, H. *Acc. Chem. Res.* **2008**, *41*, 1790–1798.
- (28) Omer, K. M.; Ku, S.-Y.; Cheng, J.-Z.; Chou, S.-H.; Wong, K.-T.; Bard, A. J. *J. Am. Chem. Soc.* **2011**, *133*, 5492–5499.
- (29) Suk, J.; Wu, Z.; Wang, L.; Bard, A. J. *J. Am. Chem. Soc.* **2011**, *133*, 14675–14685.
- (30) Kubo, R.; Kawabata, A.; Kobayashi, S. *Annu. Rev. Mater. Sci.* **1984**, *14*, 49–66.
- (31) Rossetti, R.; Ellison, J. L.; Gibson, J. M.; Brus, L. E. *J. Chem. Phys.* **1984**, *80*, 4464–4469.
- (32) Hanamura, E. *Phys. Rev. B* **1988**, *38*, 1228–1234.
- (33) Medintz, I. L.; Uyeda, H. T.; Goldman, E. R.; Mattoussi, H. *Nat. Mater.* **2005**, *4*, 435–446.
- (34) Saleh, S. M.; Ali, R.; Wolfbeis, O. S. *Chem.—Eur. J.* **2010**, *17*, 14611–14617.
- (35) Santhosh, K.; Patra, S.; Soumya, S.; Khara, D. C.; Samanta, A. *ChemPhysChem* **2011**, *12*, 2735–2741.
- (36) Galian, R. E.; Scaiano, J. C. *Photochem. Photobiol. Sci.* **2009**, *8*, 70–74.
- (37) Wu, M. Y.; Mukherjee, P.; Lamont, D. N.; Waldeck, D. H. *J. Phys. Chem. C* **2010**, *114*, 5751–5759.
- (38) Galian, R. E.; Scaiano, J. C. *Photochem. Photobiol. Sci.* **2009**, *8*, 70–74.
- (39) Landes, C. F.; Braun, M.; El-Sayed, M. A. *J. Phys. Chem. B* **2001**, *105*, 10554–10558.
- (40) Sartin, M. M.; Shu, C. F.; Bard, A. J. *J. Am. Chem. Soc.* **2008**, *130*, 5354–5360.
- (41) Shen, M.; Bard, A. J. *J. Am. Chem. Soc.* **2011**, *133*, 15737–15742.
- (42) Wallace, W. L.; Bard, A. J. *J. Phys. Chem.* **1979**, *83*, 1350–1357.
- (43) Miao, W. In *Handbook of Electrochemistry*; Zoski, C. G., Ed.; Elsevier: Oxford, UK, 2007; p 568.
- (44) Seixas de Melo, J.; Pina, J.; Burrows, H. D.; Di Paolo, R. E.; Maçanita, A. L. *Chem. Phys.* **2006**, *330*, 449–456.
- (45) Narwark, O.; Meskers, S. C. J.; Peetz, R.; Thorn-Csányi, E.; Bäessler, H. *Chem. Phys.* **2003**, *294*, 1–15.
- (46) Kim, I. T.; Lee, S. W.; Kim, S. Y.; Lee, J. S.; Park, G. B.; Lee, S. H.; Kang, S. K.; Kang, J.-G.; Park, C.; Jin, S.-H. *Synth. Met.* **2008**, *156*, 38–41.
- (47) Gierschner, J.; Egelhaaf, H.-J.; Mack, H.-G.; Oelkrug, D.; Alvarez, R. M.; Hanack, M. *Synth. Met.* **2003**, *137*, 1449–1450.
- (48) Stern, O.; Volmer, M. *Phys. Z.* **1919**, *20*, 183.
- (49) Keizer, J. *J. Am. Chem. Soc.* **1983**, *105*, 1494–1498.
- (50) Lakowicz, J. R. *Principles of Fluorescence Spectroscopy*, 3rd ed.; Springer Science + Business Media: New York, 2006.
- (51) Eftink, M. R.; Ghiron, C. A. *Anal. Biochem.* **1981**, *114*, 199–227.
- (52) Jett, E. R.; West, W. *Proc. R. Soc. London Ser. A* **1928**, *121*, 299–312.
- (53) Frank, I. M.; Wawilow, S. I. *Phys. Z.* **1931**, *69*, 100–110.
- (54) Rollefson, G. K.; Boaz, H. *J. Phys. Colloid. Chem.* **1948**, *52*, 518–527.
- (55) Boza, H.; Rollefson, G. K. *J. Am. Chem. Soc.* **1950**, *72*, 3435–3443.
- (56) Bowen, E. J.; Metcalf, W. S. *Proc. R. Soc. London Ser. A* **1950**, *206*, 437–447.
- (57) Lakowicz, R.; Weber, G. *Biochemistry* **1973**, *12*, 4161–4170.
- (58) Laws, W. R.; Contino, P. B. *Methods Enzymol.* **1992**, *210*, 448–463.
- (59) Zeng, H.; Durocher, G. *J. Lumin.* **1995**, *63*, 75–84.